

Synthesis, X-ray Structures, and Solution Properties of Vanadium(III) and -(IV) Complexes with *N*-(2-Hydroxyphenyl)-*N*-(2-pyridylmethyl)amine

Kan Kanamori,*[1] Koji Kusajima,[1] Hiroyuki Yachi,[1] Honoh Suzuki,[1] Yoshitaro Miyashita,[2] and Ken-ichi Okamoto[2]

[1]Department of Chemistry, Faculty of Science, University of Toyama, Gofuku 3190, Toyama 930-8555

[2]Department of Chemistry, Graduate School of Pure and Applied Sciences, University of Tsukuba, Tsukuba 305-8571

Received March 9, 2006; E-mail: kanamori@sci.u-toyama.ac.jp

New vanadium(III) and -(IV) complexes with *N*-(2-hydroxyphenyl)-*N*-(2-pyridylmethyl)amine (H_2hppma) have been prepared, and their structures have been determined by X-ray crystallography. As for the vanadium(III) complex, the vanadium(III) center has a center of symmetry and adopts an ordinary octahedral structure, in which the H_2hppma ligand coordinates as a monoanion (Hhppma) in a facial fashion. The vanadium(IV) complex with H_2hppma has been determined to be an unusual non-oxo or bare vanadium(IV) complex. In this complex, the H_2hppma ligand coordinates as a dianion (hppma) in a meridional fashion. Both complexes are fairly unstable in an aerobic solution and decompose to an oxovanadium(IV) complex.

Recently, interest in vanadium chemistry and biology has been increasing.[1–4] Vanadium compounds can adopt a wide variety of oxidation states from −I to +V, of which +III, +IV, and +V states exist in biological systems. In order to further the understanding of the biological aspects of vanadium, it is important to obtain more information concerning the properties of vanadium(III), -(IV), and -(V) complexes coordinated by biologically relevant functional groups. One of the most interesting physiological activities of vanadium is its insulin-mimetic activity.[5] With regard to the insulin-mimetic behavior of vanadium, the interaction between vanadium and the tyrosine residues of the insulin receptor is believed to play an important role. It has been suggested that vanadate(V) and oxovanadium(IV) inhibit protein phosphotyrosine phosphatase (PPTP) that is selective for cytosolic protein tyrosine kinase (cytPTK) rather than the PPTP that targets insulin recepter kinase (IRK).[6,7] However, the study of phenolato–vanadium complexes that can be regarded as model compounds for the interaction between vanadium and tyrosine residue of proteins is relatively sparse especially for the lower valent vanadium ions.[8,9]

In small model complexes with tyrosine itself or dipeptides containing tyrosine residue, it is very difficult to obtain a complex coordinated via the phenolato group of tyrosine. This difficulty mainly comes from a steric requirement, that is, preferential chelate formation through the terminal carboxylate and the terminal amino groups as well as the amide nitrogen of dipeptides leaves the *p*-hydroxyphenyl group in the side arm uncoordinated.[10–12] We employed here a tridentate ligand containing a hydroxyphenyl group as shown in Scheme 1 in order to examine the structure and properties of vanadium(III) and -(IV) complexes coordinated through phenolato oxygen. A soft pyridyl functionality was introduced to stabilize the lower valent vanadium. In this paper, we report the syntheses, X-ray structures, and solution properties of vanadium(III) and -(IV) complexes containing a tridentate ligand *N*-(2-hydroxyphenyl)-*N*-(2-pyridylmethyl)amine (H_2hppma).

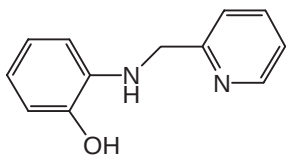

H2hppma

Scheme 1.

Experimental

Compound Preparations. Reagents were obtained from commercial source and used without further purification. All of the synthetic procedure for the vanadium complexes were performed under an Ar atmosphere using standard Schlenk techniques or in a N_2-filled glove box.

***N*-(2-Hydroxyphenyl)-*N*-(2-pyridylmethyl)amine (H_2hppma).** H_2hppma (Scheme 1) was prepared according to a general method using *o*-aminophenol and 2-pyridinecarboaldehyde.[13]

$[V^{III}(Hhppma)_2]Cl\cdot 3H_2O$. An aqueous solution (10 cm^3) of vanadium(III) chloride (0.16 g, 1.0 mmol) was mixed with a methanolic solution (20 cm^3) of H_2hppma (0.40 g, 2.0 mmol). To the solution was added $LiOH\cdot H_2O$ (0.08 g, 2 mmol). Allowing the resulting dark green solution to stand for a long time afforded brown crystals. Yield 61%. Anal. Calcd for $C_{24}H_{28}N_4O_5ClV$ ($[V^{III}(Hhppma)_2]Cl\cdot 3H_2O$): C, 53.33; H, 5.18; N, 10.37%. Found: C, 53.51; H, 5.19; N, 10.40%. Selected IR data (KBr disk): 1611, 1591, 1484, 1452, 1260, 1028, 853, 766, 639 cm^{-1}.

$[V^{IV}(hppma)_2]$. Vanadium(IV) oxide sulfate trihydrate (0.22 g, 1.0 mmol) and barium perchlorate (0.34 g, 1.0 mmol) were mixed in 20 cm^3 of water. Barium sulfate, which precipitated, was removed by filtration. The resulting blue solution was mixed

Published on the web February 13, 2007; doi:10.1246/bcsj.80.324

Table 1. Summary of X-ray Data Collection and Refinement

	$[V^{III}(Hhppma)_2]Cl\cdot 3H_2O$	$[V^{IV}(hppma)_2]$
Empirical formula	$C_{24}H_{28}N_4O_5ClV$	$C_{24}H_{20}N_4O_2V$
Formula weight	538.89	447.39
Crystal system	Triclinic	Triclinic
Space group	$P\bar{1}$	$P\bar{1}$
a/Å	9.507(2)	12.952(5)
b/Å	14.307(7)	15.445(6)
c/Å	9.456(3)	11.143(4)
α/°	92.45(3)	93.70(3)
β/°	94.02(2)	114.65(3)
γ/°	91.96(3)	86.96(3)
V/Å^3	1280.9(8)	2020(1)
Z	2	4
T/K	296	296
ρ_{calcd}/g cm^{-3}	1.397	1.470
λ(Mo Kα)/Å	0.7107	0.7107
μ (Mo Kα)/cm^{-1}	5.33	5.21
F(000)	560	924
No. of measured reflns	7875	12246
No. of unique reflns	7456	11764
No. of obsd reflns	3602 ($I > 2\sigma(I)$)	8103 ($I > 3\sigma(I)$)
No. of params	337	559
R, Rw	0.069, 0.186	0.047, 0.099
GOF	0.974	1.31

with a methanolic solution (20 cm^3) of H_2hppma (0.40 g, 2.0 mmol) to give a dark green solution. Allowing the solution to stand at room temperature afforded dark brown crystals. Yield 28%. Anal. Calcd for $C_{24}H_{20}N_4O_2V$ ($[V^{IV}(hppma)_2]$): C, 64.43; H, 4.51; N, 12.53%. Found: C, 64.42; H, 4.46; N, 12.40%. Selected IR data (KBr disk): 1608, 1567, 1483, 1462, 1295, 1281, 1124, 1074, 1019, 768, 738, 615, 526 cm^{-1}.

Decomposition Product. $[V^{IV}(hppma)_2]$ was found to be unstable in air. Allowing the reaction solution obtained as above to stand under aerobic conditions yielded a dark brown powder. Yield 9.4%. Anal. Calcd for $C_{12.5}H_{12}N_2O_{2.5}V$ (VO(hppma)$\cdot$ 0.5CH_3OH): C, 53.40; H, 4.31; N, 9.96%. Found: C, 53.87; H, 4.28; N, 9.82%. Selected IR data (KBr disk): 1588, 1482, 1460, 1295, 1278, 1263, 1243, 1187, 1089, 969 (ν(V=O)), 862, 780, 624 cm^{-1}.

Measurements. UV–vis spectra were measured using a Shimadzu UV-3100PC spectrophotometer. Infrared spectra were recorded on a JASCO FT/IR-8000S. EPR spectra were obtained with a JEOL JES-RE1XESR spectrometer.

X-ray Structure Determination. The crystallographic data are summarized in Table 1. Crystals were mounted on a glass fiber, coated with epoxy resin as a precaution against solvent loss, and centered on a Rigaku AFC7R diffractometer using graphite-monochromated Mo Kα radiation. Data reduction and the application of Lorentz, polarization, linear decay correction, and empirical absorption corrections based on a series of psi-scans were carried out. The structure was solved by direct methods, that is, SHELXS97[14] for the V^{III} complex or SIR92[15] for the V^{IV} complex, and expanded using Fourier techniques, that is, SHELXL97[16] for the V^{III} complex or DIRDIF94[17] for the V^{IV} complex. The structures were refined by full-matrix least-squares techniques on F^2. All non-hydrogen atoms were refined anisotropically. For the vanadium(III) complex, the fraction of observed reflections was relatively small, which is a possible reason for the larger R factor. All calculation were performed using SHELX97[18] for the V^{III} complex or teXsan[19] for the V^{IV} complex. The CIF files have been deposited with CCDC 619285 and 619286. Copies of the data can be obtained on request free of charge by quoting the publication citation and the deposition number via http://www.ccdc.cam.ac.uk/conts/retrieving.html (or from the Cambridge Crystallographic Data Centre, 12, Union Road, Cambridge, CB2 1EZ, UK; Fax: +44 1223 336033; e-mail: deposit@ccdc.cam.ac.uk).

Results and Discussion

X-ray Structures. The selected bond distances and angles are summarized in Table 2. A perspective view of $[V^{III}(Hhppma)_2]^+$ is shown in Fig. 1 with its numbering scheme. The unit cell contains two crystallographically independent complex ions; however, their geometry and dimensions are almost the same. The vanadium(III) complex adopts an ordinary octahedral structure with two crystallographically equivalent ligands and has a center of inversion on the vanadium(III) ion, resulting in an all trans configuration. As a consequence of the inversion center, two asymmetric nitrogen atoms in the tridentate ligands inevitably take opposite absolute configurations with each other. Thus, the complex is achiral with regard to the chelate ring arrangement as well as the asymmetric nitrogen. The tridentate ligand H_2hppma coordinates as a monoanion, Hhppma, in a facial fashion through the deprotonated phenolato group, the amine nitrogen, and the pyridyl nitrogen. The bond distances and angles are in the normal range.

The unit cell of the vanadium(IV) complex with hppma contains two crystallographically independent complex ions, although their geometry and dimensions are almost the same as in the case of the vanadium(III) complex. Figure 2 shows a perspective view of one of the independent complexes in the unit cell. The chemistry of vanadium(IV) is dominated by the oxovanadium, VO^{2+}, ion with a few exceptions of non-oxo or bare vanadium(IV) species, such as tris(phenolato) complexes[20–22] and a Schiff-base complex.[23] Amavadine, which is present in some *Amanita* fungi, is a natural non-oxo vanandium(IV) complex coordinated by (*S*,*S*)-2,2′-(hydroxyimino)-dipropionate.[24] As can be seen in Fig. 2, the vanadium(IV) complex with H_2hppma is a new example of a non-oxo or bare vanadium(IV) complex. The absence of V=O stretching in the IR spectrum is consistent with this structure. In addition to the unusual bare vanadium(IV) structure, the vanadium(IV)–hppma complex has some other notable characteristics. First, the H_2hppma ligand coordinates to the vanandium(IV) center as a dianion (hppma) through the deprotonated phenolato group, the deprotonated amino group, and the pyridyl group. The deprotonation of the amino group is confirmed by the charge balance within the complex and the geometry around the amino nitrogen atom. The bond angles around the nitrogen atom (N1a) are near to 120° (V1a–N1a–C7a = 123.8°, C6a–N1a–C7a = 118.4°, V1a–N1a–C6a = 117.5°) indicating sp^2 hybridization for the N atom. Second, the increased basicity due to the deprotonation is reflected in the very short V–N(amine) bond length (av. 1.946 Å) compared to av. 2.151 Å of the vanadium(III) complex. The other coordinating bond lengths are comparable to the corresponding ones in the vana-

Table 2. Selected Bond Distances (Å) and Angles (°) for $[V^{III}(Hhppma)_2]Cl\cdot 3H_2O$ and $[V^{IV}(hppma)_2]$[a)]

$[V^{III}(Hhppma)_2]Cl\cdot 3H_2O$		$[V^{IV}(hppma)_2]$	
V1a–O1a	1.928(3)	V1a–O1a	1.960(1)
V1b–O1b	1.916(3)	V1b–O1b	1.952(1)
		V1a–O2a	1.949(1)
		V1b–O2b	1.951(1)
V1a–N1a	2.146(3)	V1a–N1a	1.942(2)
V1b–N1b	2.155(3)	V1b–N1b	1.946(2)
		V1a–N3a	1.949(2)
		V1b–N3b	1.946(2)
V1a–N2a	2.131(3)	V1a–N2a	2.137(2)
V1b–N2b	2.145(3)	V1b–N2b	2.122(2)
		V1a–N4a	2.102(2)
		V1b–N4b	2.128(2)
O1a–V1a–O1a(i)	180.0	O1a–V1a–O2a	97.42(6)
O1b–V1b–O1b(i)	180.0	O1b–V1b–O2b	97.61(6)
O1a–V1a–N1a	83.14(11)	O1a–V1a–N1a	79.25(6)
O1b–V1b–N1b	83.10(12)	O1b–V1b–N1b	79.25(6)
O1a–V1a–N2a	91.19(12)	O1a–V1a–N2a	154.83(6)
O1b–V1b–N2b	92.22(13)	O1b–V1b–N2b	155.69(6)
O1a–V1a–N1a(i)	96.86(11)	O1a–V1a–N3a	111.11(6)
O1b–V1b–N2b(i)	96.90(12)	O1b–V1b–N3b	107.98(6)
O1a–V1a–N2a(i)	88.81(12)	O1a–V1a–N4a	88.40(6)
O1b–V1b–N2b(i)	87.78(13)	O1b–V1b–N4b	89.61(6)
		O2a–V1a–N1a	106.01(6)
		O2b–V1b–N1b	106.89(6)
		O2a–V1a–N2a	94.21(6)
		O2b–V1b–N2b	89.67(6)
		O2a–V1a–N3a	79.10(6)
		O2b–V1b–N3b	79.20(6)
		O2a–V1a–N4a	155.48(6)
		O2b–V1b–N4b	155.26(6)
N1a–V1a–N2a	77.50(12)	N1a–V1a–N2a	76.11(6)
N1b–V1b–N2b	76.98(13)	N1b–V1b–N2b	76.44(6)
N1a–V1a–N1a(i)	180.0	N1a–V1a–N3a	168.10(6)
N1b–V1b–N1b(i)	180.0	N1b–V1b–N3b	170.15(7)
N1a–V1a–N2a(i)	102.50(12)	N1a–V1a–N4a	98.47(6)
N1b–V1b–N2b(i)	103.02(13)	N1b–V1b–N4b	97.68(6)
		N2a–V1a–N3a	92.95(6)
		N2b–V1b–N3b	96.14(6)
N2a–V1a–N2a(i)	180.0	N2a–V1a–N4a	90.21(6)
N2b–V1b–N2b(i)	180.0	N2b–V1b–N4b	93.39(6)
		N3a–V1a–N4a	76.60(6)
		N3b–V1b–N4b	76.07(6)

a) Symmetry operation: (i) $-x$, $-y$, $-z$.

dium(III) complex. Coordination through a deprotonated amide nitrogen has been found in the dipeptide–oxovanadium(IV) complex,[25] of which the V–N(amide) bond length (1.997(4) Å) is slightly longer than the V–N(amine) bond length in the present complex. It is of interest to note that H_2hppma coordinates to vanadium(IV) ion as a dianion in spite of the absence of base in the preparation.

$$V^{IV}O^{2+} + 2H_2hppma \rightarrow [V^{IV}(hppma)_2] + H_2O + 2H^+$$

Finally, the deprotonation of the amine nitrogen also changes the coordination mode of the tridentate ligand. In other words, hppma coordinates to the vanadium center in a meridional fashion, whereas Hhppma coordinates in a facial fashion. This result is surprising in view of the fact that the meridional coordination constrains the vanadium(IV) center to adopt a significantly distorted environment for the vanadium(IV) center represented by the very small trans angles in the octahedron (av. O1–V1–N2 = 155.28° and av. O2–V1–N4 = 155.37°). The bite angles of the chelate rings are comparable to those in the vanadium(III) complex.

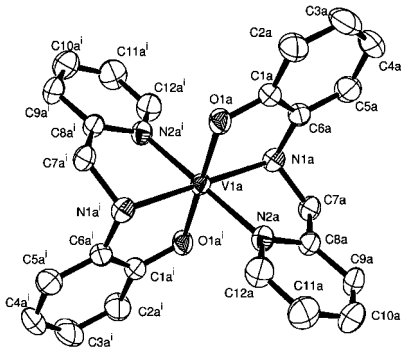

Fig. 1. ORTEP of $[V^{III}(Hhppma)_2]^+$.

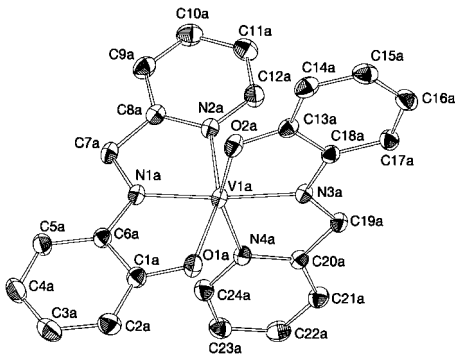

Fig. 2. ORTEP of $[V^{IV}(hppma)_2]$.

Absorption Spectra and Solution Properties. The UV–vis absorption spectrum of $[V^{III}(Hhppma)_2]Cl$ in methanol/water, shown in Fig. 3, consists of two distinct absorption bands at 378 (ε/cm^{-1} mol^{-1} dm^3 = 2510) and 660 nm (ε = 765) with the shoulders around 330 and 550 nm. It has been reported that $[V^{III}$\{1,4,7-tris(5-*t*-butyl-2-hydroxybenzyl)-1,4,7-triazacyclononane\}] exhibits absorption bands at 360 (ε = 4550) and 540 nm (ε = 3700).[21] Both bands have been assigned to phenolate-to-vanadium(III) charge-transfer (CT) transitions. For the present vanadium(III) complex, the band at 378 nm can be assigned unequivocally to a CT transition, while the intensity of the band at 660 nm is rather low for a CT transition but much higher than an ordinary d–d transition. We, therefore, tentatively assigned the 660-nm band to a d–d transition, of which intensity is borrowed from a CT transition.

The UV–vis absorption spectrum of $[V^{IV}(hppma)]$ (Fig. 3)

Although it is difficult to point out unequivocally the properties of the ligand required for non-oxo vanadium(IV) complexes, ligands containing a phenol functionality have a tendency to yield non-oxo vanadium(IV) complexes.[20–22] Klich et al. have stated that ligands stabilizing the non-oxo vanadium(IV) complexes must have the ability to donate sufficient electron density (σ and π) to the metal.[22] The present ligand hppma seems to satisfy this requirement.

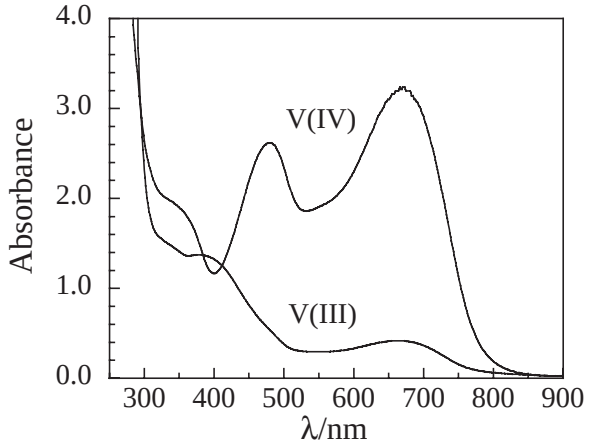

Fig. 3. UV–vis spectra of the H_2hppma complexes under unaerobic condition: Lower, $[V^{III}(Hhppma)_2]Cl\cdot 3H_2O$; $[V^{3+}] = 0.54\,mmol\,dm^{-3}$; solvent, MeOH/$H_2O$ (1:1). Upper, $[V^{IV}(hppma)_2]$; $[V^{4+}] = 0.50\,mmol\,dm^{-3}$, solvent, MeOH.

exhibits very intense bands in the visible region: λ_{max}/nm (ε/$cm^{-1}\,mol^{-1}\,dm^3$), 480 (5220); 666 (6480). Similar intense visible bands have been observed for the bare vanadium(IV) complexes coordinated by phenolato group and have been assigned to the phenolate-to-vanadium(IV) charge-transfer transitions.[20,21] A similar assignment can also be made for the present complex.

In the preparation of $[V^{III}(Hhppma)_2]Cl$, dark brown crystals sometimes deposited in addition to brown crystals of the desired complex. The dark brown crystals were found to be an oxidized species, namely $[V^{IV}(hppma)_2]$. The color of a solution of the vanadium(IV) complex readily changed on exposure to air. These observations indicate that the present vanadium(III) and -(IV) complexes in solution are very sensitive toward air oxidation, though both complexes in the crystalline state are fairly stable even in air. We, therefore, examined the time dependence of the absorption spectrum of the vanadium(III) complex as well as the vanadium(IV) complex under aerobic conditions. The results are shown in Figs. 4 and 5, respectively. As for the vanadium(IV) complex, the intensities of the bands at 480 and 666 nm rapidly decreased with time while new bands appeared at 333 and 460 nm (see Fig. 5). The spectrum stopped changing after about 2 h.

In order to characterize the decomposition product, EPR spectrum of the solution after decomposition was measured. The observed spectrum is shown in Fig. 6 with that of $[V^{IV}(hppma)_2]$. The EPR spectrum of $[V^{IV}(hppma)_2]$ at ambient temperature (Fig. 6A) displayed the typical eight-line pattern for vanadium(IV) complexes (^{51}V, $I = 7/2$; $g_0 = 1.975$, $A_0 = 81 \times 10^{-4}\,cm^{-1}$). The EPR spectrum of the solution after decomposition (Fig. 6B) still exhibited the characteristic pattern for vanadium(IV) complexes ($g_0 = 1.981$, $A_0 = 101 \times 10^{-4}\,cm^{-1}$). The hyperfine values are known to be sensitive to changes in the coordination sphere.[20] The increase in the A_0 values was also observed for the structural change from the non-oxo complex $[V(cat)_3]^{2-}$ (cat = catecolate) ($A_0 = 75 \times 10^{-4}\,cm^{-1}$) to the oxo complex $[VO(cat)_2]^{2-}$ ($A_0 = 82 \times 10^{-4}\,cm^{-1}$).[20] The final decomposition product is, therefore

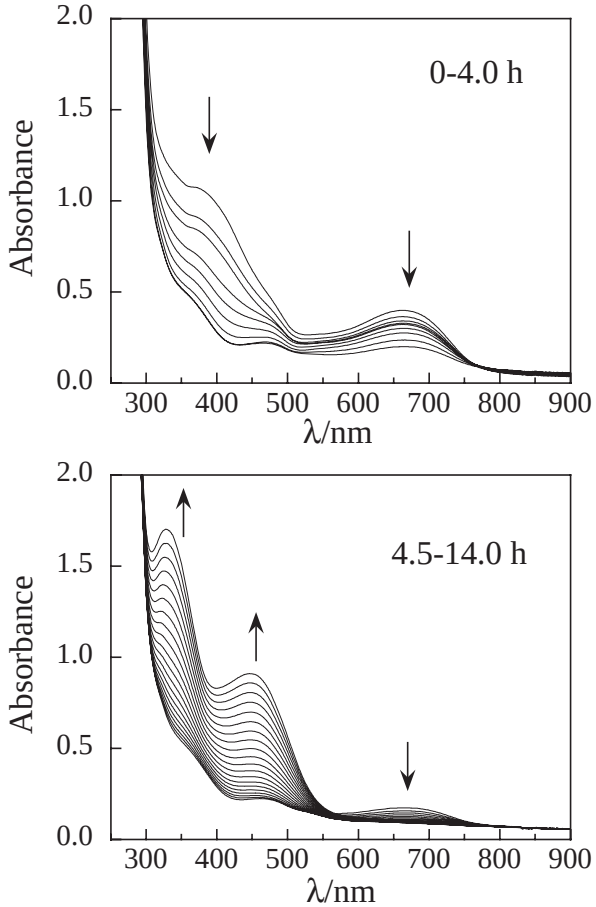

Fig. 4. Time-dependent UV–vis spectra of $[V^{III}(Hhppma)_2]Cl\cdot 3H_2O$ under aerobic condition: $[V^{3+}] = 0.54\,mmol\,dm^{-3}$; every 30 min.

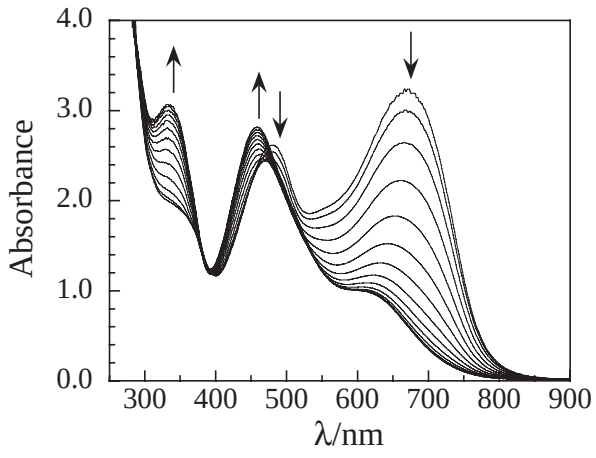

Fig. 5. Time-dependent UV–vis spectra of $[V^{IV}(hppma)_2]$ under aerobic condition: $[V^{4+}] = 0.50\,mmol\,dm^{-3}$, every 5 min.

considered to be an oxovanadium(IV) species. A dark brown powder that exhibited the same EPR spectrum as Fig. 6B was isolated from the solution after decomposition. Elemental analysis suggested that this dark brown complex is $V^{IV}O(hppma)\cdot 0.5CH_3OH$. The IR spectrum of this compound exhibited a band at 969 cm^{-1} that is assigned to ν(V=O), while

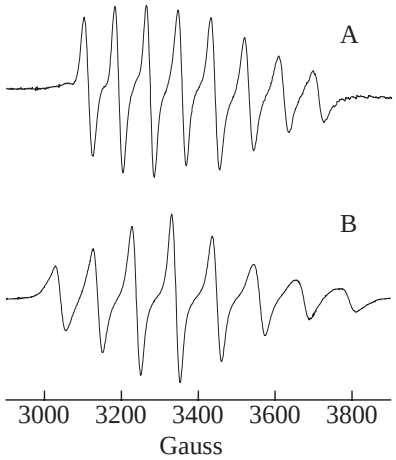

Fig. 6. EPR spectra: A, $[V^{IV}(hppma)_2]$ in $MeOH/H_2O$; B, the solution after decomposition.

the IR band was absent in this region for $[V^{IV}(hppma)_2]$ (see Experimental Section). In addition, it was found that a solution prepared by mixing V^V and H_2hppma exhibited absorption and EPR spectra very similar to those of the final decomposition product, suggesting the reduction of V^V to V^{IV} by free H_2hppma. These results indicates that $[V^{IV}(hppma)_2]$ decomposed to an oxovanadium(IV) complex with one hppma ligand, which is supposed to be the most stable form of the V/H_2hppma system under aerobic conditions. The possibility that $[V^{IV}(hppma)_2]$ was first oxidized to V^V species followed by reduction due to a dissociated hppma ligand can not be ruled out at present.

The absorption spectrum of $[V^{III}(Hhppma)_2]Cl$ in an aerobic solution changed stepwise as shown in Fig. 4. Namely the intensities of the bands at 378 and 660 nm diminished with time over a 4 h period. Accompanying this spectral change, new bands at 480 and 666 nm and a shoulder around 380 nm appeared. The spectral features observed after 4 h resembled that of $[V^{IV}(hppma)_2]$ though the intensities of the new bands were low compared to those observed for the authentic vanadium(IV) complex. After 4.5 h, the band at 666 nm completely disappeared, and bands at 333 and 460 nm grew, approaching the final spectrum observed for the time-dependence of the absorption spectrum of $[V^{IV}(hppma)_2]$. These observations suggest that under an aerobic conditions, $[V^{III}(Hhppma)_2]^+$ was oxidized to the oxovanadium(IV) species via non-oxo $[V^{IV}(hppma)_2]$, but the intermediate non-oxo vanadium(IV) complex did not accumulate in the oxidation process of the vanadium(III) complex because of rapid decomposition to the oxovanadium(IV) species.

In summary, it has been found that in spite of the introduction of a pyridyl group as a soft donor in the chelate ligand to stabilize vanadium(III) state, a hard phenolato group governs the redox properties of vanadium complex. As a consequence, the vanadium(III) complex is easily oxidized to vanadium(IV) species.

References

1 *Vanadium in Biological Systems*, ed. by N. D. Chasteen, Kluwer Academic Publishers, Dordrecht, **1990**.

2 *Vanadium and Its Role in Life* in *Metal Ions in Biological Systems*, ed. by H. Sigel, A. Sigel, Marcel Dekker, New York, **1995**, Vol. 31.

3 *Vanadium in the Environment Advances in Environmental Science and Technology*, ed. by J. O. Nriagu, John Wiley & Sons, New York, **1998**, Vol. 30.

4 Special Issue: New Direction in Chemistry and Biological Chemistry of Vanadium: *Coord. Chem. Rev.* **2003**, *237*.

5 H. Sakurai, A. Tsuji, *Vanadium in the Environment, Part 2. Health Effects Advances in Environmental Science and Technology*, ed. by J. O. Nriagu, John Wiley & Sons, New York, **1998**, Vol. 30, pp. 297–315.

6 Y. Shechter, J. Meyerovitch, Z. Farfel, J. Farfel, J. Sack, R. Bruck, S. Bar-Meir, S. Amir, H. Degani, S. J. D. Karlish, *Vanadium in Biological Systems*, ed. by N. D. Chasteen, Kluwer Academic Publishers, Dordrecht, **1990**, pp. 129–142.

7 C. Slebodnick, B. J. Hamstra, V. L. Pecoraro, *Struct. Bonding (Berlin)* **1997**, *89*, 51.

8 A. S. Tracey, M. J. Gresser, *Proc. Natl. Acad. Sci. U.S.A.* **1986**, *83*, 609.

9 M. Ebel, D. Rehder, *Inorg. Chim. Acta* **2003**, *356*, 210.

10 A. S. Tracey, J. S. Jaswal, F. Nxumalo, S. J. Angus-Dunne, *Can. J. Chem.* **1995**, *73*, 489.

11 D. C. Crans, H. Holst, A. D. Keramidas, D. Rehder, *Inorg. Chem.* **1995**, *34*, 2524.

12 A. J. Tasiopoulos, Y. G. Deliginnakis, J. D. Woollins, A. M. Z. Slawin, T. A. Kabanos, *Chem. Commun.* **1998**, 569.

13 S. Ogo, R. Yamahara, T. Funabiki, H. Masuda, Y. Watanabe, *Chem. Lett.* **2001**, 1062.

14 G. M. Sheldrick, *SHELXS97*, University of Göttingen, Germany, **1997**.

15 A. Altomare, M. C. Burla, M. Camalli, M. Cascarano, C. Giacovazzo, A. Guagliardi, G. Polidori, *J. Appl. Crystallogr.* **1994**, *27*, 435.

16 G. M. Sheldrick, *SHELXL97*, University of Göttingen, Germany, **1997**.

17 P. T. Beyrskens, G. Admiraal, G. Beurskens, W. P. Bosman, R. de Gelder, R. Israel, J. M. M. Smith, *The DIRDIF-94 Program System, Technical Report of the Crystallography Laboratory*, University of Nijmegen, The Netherlands, **1994**.

18 G. M. Sheldrick, *SHELX97*, University of Göttingen, Germany, **1997**.

19 teXsan: *Crystal Structure Analysis Package, Ver. 1.10*, Molecular Structure Corporation, **1985** and **1999**.

20 S. R. Cooper, Y. B. Koh, K. N. Raymond, *J. Am. Chem. Soc.* **1982**, *104*, 5092.

21 U. Auerbach, B. S. P. C. D. Vedova, K. Wieghardt, B. Nuber, J. Weiss, *J. Chem. Soc., Chem. Commun.* **1990**, 1004.

22 P. R. Klich, A. T. Daniher, P. R. Challen, D. B. McConville, W. Y. Youngs, *Inorg. Chem.* **1996**, *35*, 347.

23 H. Hefele, E. Ludwig, E. Uhlemann, F. Weller, *Z. Anorg. Allg. Chem.* **1995**, *621*, 1973.

24 a) E. Bayer, H. Kneifel, *Z. Naturforsch., B: Chem. Sci.* **1972**, *27*, 207. b) E. Bayer, E. Koch, G. Anderegg, *Angew. Chem., Int. Ed. Engl.* **1987**, *26*, 545. c) M. A. A. F. de C. T. Carrondo, M. T. L. S. Duarte, J. C. Pessoa, J. A. L. Silva, J. J. R. Fraústo da Silva, M. C. T. A. Vaz, L. F. Vilas-Boas, *J. Chem. Soc., Chem. Commun.* **1988**, 1158.

25 A. J. Tasiopoulos, A. T. Vlahos, A. D. Keramidas, T. A. Kabanos, Y. G. Deligiannakis, C. P. Raptopoulou, A. Terzis, *Angew. Chem., Int. Ed. Engl.* **1996**, *35*, 2531.